

Insights into the Encapsulation Process of Photovoltaic Modules: GC-MS Analysis on the Curing Step of Poly(ethylene-co-vinyl acetate) (EVA) Encapsulant

Heng-Yu Li^a, Ricardo Théron^{a*}, Gregory Röder^b, Ted Turlings^b, Yun Luo^c, Ronald F.M. Lange^{c#}, Christophe Ballif^a, and Laure-Emmanuelle Perret-Aebi^{a*}

^aEcole Polytechnique Fédérale de Lausanne (EPFL), Institute of Microengineering (IMT), Photovoltaics and Thin Film Electronics Laboratory, Rue A.-L. Breguet 2, CH-2000 Neuchâtel, Switzerland

^bUniversity of Neuchâtel, Institute of Biology, Fundamental and Applied Research in Chemical Ecology, Case Postale 158, CH-2009 Neuchâtel, Switzerland

^c3S Swiss Solar Systems AG, Schachenweg 24, CH-3250 Lyss, Switzerland

Received: 22 March 2012, Accepted: 23 April 2012

SUMMARY

Appropriate encapsulation schemes are essential in protecting the active components of the photovoltaic (PV) module against weathering and to ensure long term reliability. For crystalline cells, poly(ethylene-co-vinyl acetate) (EVA) is the most commonly used PV encapsulant. Additives like peroxides and silanes are formulated in EVA encapsulants to obtain the desired properties, e.g. the desired gel content value and sufficient adhesion after the encapsulation process etc. The identification and control of volatile organic compounds (VOCs) released by the polymeric encapsulant during PV module encapsulation is important for understanding and optimizing processes in order to enhance the encapsulation quality of the manufactured modules. The authors demonstrate how gas chromatography and mass spectrometry (GC-MS) techniques can be used to help understand the curing process, mainly by identifying the VOCs emanating from EVA under the effect of temperature and pressure. The results provide chemical insights into the EVA encapsulation process, which are valuable for further optimization of the PV module manufacturing process and evaluation of its environmental impact.

Keywords: Photovoltaic, Encapsulation quality, EVA, GC-MS, Environmental impact

1. INTRODUCTION

The photovoltaic (PV) industry has been experiencing unprecedented growth in recent years with newly added PV capacity of ~ 22 gigawatts (GW) worldwide in 2011¹. In PV modules, a good encapsulation scheme is essential to protect the active energy-conversion component against various stresses experienced during field deployment². In such a scheme, a polymeric PV encapsulant is commonly used as an adhesive to bond

all the components (cells, front glass, backsheet, etc) together for maintaining structural stability in the PV module. It also provides protection against natural stresses including moisture and oxygen ingress, mechanical stresses like wind/precipitation load, daily and annual thermal cycles and their cumulative degrading effects²⁻⁴. Thus, a good PV encapsulant should exhibit qualified performance in terms of optical transparency, chemical stability, electrical insulation, thermal conductivity, matching of thermal

expansion coefficients, moisture barrier properties etc.^{5,6}. Poly(ethylene-co-vinyl acetate) (EVA) has been the dominant encapsulant used in crystalline PV modules since 1980s and currently occupies nearly 80% of the PV encapsulant market⁷. EVA is a statistical copolymer consisting of ethylene and vinyl acetate (VA). The VA% of EVA encapsulants is typically 28-33%, like EVA-based adhesive in other applications. The EVA PV encapsulant is usually provided in sheet form with a sub-millimetre thickness for easy handling. To ensure its desired performance, the EVA encapsulant is specially formulated with additives like UV stabilizers, adhesion promoters, anti-oxidation agents and curing agents. In PV EVA formulation, peroxides are often used as the curing agents to initiate the crosslinking

+now with Gadir Solar, 11510 Puerto Real, Cádiz, Spain

#now with 9-om AG, Wiesenstrasse 26, CH-3073 Gümligen, Switzerland

*Corresponding author: Phone: +41 (0) 32 718 33 56; Fax: +41 (0) 32 718 32 01.

Email: laure-emmanuelle.perret@epfl.ch

©Smithers Rapra Technology, 2012

reaction and transform EVA into an elastomer⁸. The encapsulation process of crystalline PV modules is usually performed in a flat-bed vacuum-bag laminator⁹⁻¹¹. It normally includes the following steps: (i) Preheating of PV modules on metal pins while a vacuum is generated to evacuate air potentially trapped in the module lay-up. (ii) After pre-heating, the pins are removed and the PV module is directly pressed onto the heating plate by a membrane. The resulting improved heat transfer allows the lay-up temperature to rise rapidly to the desired curing temperature (140 to 160 °C). (iii) The EVA curing process is initiated by the thermally-activated peroxide once its temperature reaches the processing temperature. The EVA curing continues until the desired EVA gel-content is obtained¹¹⁻¹³. (iv) The PV module is transferred out of the lamination chamber and cools down in air or under controlled conditions.

The EVA curing process occurs at a relatively high temperature between 120 °C and 160 °C. Considering the various additives formulated in EVA, complex chemical reactions are expected to take place during the curing step. The volatile organic compounds (VOCs) produced therein is probably one of the possible origins of the voids observed inside the EVA layer in the PV modules after encapsulation, as suggested for the autoclave or vacuum-bag processing of thermoset composites¹⁴⁻¹⁶. Furthermore, the VOCs produced in the encapsulation process of PV modules may also possess environmental impacts or harm the components of laminators, which seem to have been overlooked in previous work. To our knowledge, there is little information available in the published literature on how to optimize the encapsulation process, based on GC-MS study of the chemical processes occurring during PV module encapsulation¹⁷⁻²⁰. In this paper, we demonstrate the application of GC-MS technique for tracking the encapsulation process, more precisely the EVA curing process, by analysis of the VOCs released from the process upon heating.

For this purpose, a static approach is taken in which the volatiles are collected by heating the EVA samples in glass vials. This can effectively simulate the temperature and residence time (major influential factors on VOC emission rate) that EVA experiences in the actual encapsulation process in the laminator while avoiding possible contaminations from the laminator. The results obtained by this study can help understanding of the chemical reactions occurring during EVA encapsulation, which is essential in improving the manufacturing process of PV modules.

2. EXPERIMENTAL

The GC-MS data were acquired by a gas chromatograph (Agilent 7890A) and a mass spectrometer (Agilent 5975C) with a robotic sampler (Gerstel MPS 2). The system was equipped with a Gerstel Thermal Desorption Unit (TDU) and Gerstel Cooled Injection System (CIS). The analyzed samples were placed in micro-vial inserts and liners (Gerstel) used for thermal extraction in the TDU. Samples of 5 mg of a commercially available fast-cure EVA were prepared for the GC-MS analysis. The effused gases from the thermal decomposition of EVA were collected *via* a head-space system. The VOC collection temperature ranged from 20 to 160 °C with steps of 20 °C. At each temperature, the VOCs were collected during 5 minutes. 7-tridecanone is used as an internal standard for estimating the quantities of various VOCs.

2.1 Analysis Conditions

The samples were thermally extracted in a TDU, followed by injection into the column with a CIS. The TDU was operated in splitless mode. The TDU temperature program for extraction was 20 °C (hold for 2 min), followed by a 640 °C/min ramp to 20/40/60/80/100/120/140/160 °C (depending on the sample), and then a hold time of 5 minutes at the final temperature. The CIS was cooled with liquid nitrogen to -80 °C. After

extraction and cryo-trapping, the CIS was heated at 12 °C/s to 280 °C, with hold time of 10 min. The CIS inlet was operated in the solvent vent mode, a vent pressure of 14 psi, a vent flow of 50 mL/min, and a purge flow of 50 mL/min. Separation was performed by a HP-1MS (30 m length x 0.25 mm i.d., 0.25 μm film thickness) capillary column from Agilent. The temperature program of the GC operation was 50 °C for 1 min, an increase to 200 °C at a rate of 5 °C/min (hold time 10 min), followed by a second ramp at a rate of 100 °C/min to 250 °C (hold time 2 min), and finally a 3 min post run at 50 °C. The helium carrier gas pressure was 14 psi (flow rate 0.7 mL/min) in constant flow mode. A MSD transfer line temperature was set at 280 °C. The ion source and quadrupole temperatures were set at 230 °C and 150 °C respectively. Electron impact (EI) mode was used with a scan over the mass range of 35-350.

3. RESULTS AND DISCUSSION

During the PV module encapsulation process a crosslinked polymeric matrix is obtained in the bulk EVA after the curing step. This process provides the desired thermo-mechanical and optical properties to the EVA, which ensures high-quality packaging². In this section, the nature of the VOCs generated by the EVA encapsulant at various temperatures is studied at first. Then the chemical processes involved in module encapsulation are proposed based on the GC-MS analysis. The actual crosslinking and adhesion reactions during the encapsulation process are illustrated thereafter. At last, the environmental impact of VOCs produced is the PV module encapsulation process is discussed.

3.1 GC-MS study

A typical GC-MS chromatogram from EVA after 5 min collection at 160 °C is presented in **Figure 1**. The major peaks on the chromatogram correspond to light hydrocarbons, aldehydes, the direct

reaction products of the peroxide, and the adhesion promoter or the antioxidant agents among other additives present in the EVA formulation, respectively. The broad peak at 1.2 min (as seen in the insert) corresponds to tert-butanol according to mass spectrometry. It is not very well resolved, but can probably be improved by changing the chromatographic method or the column.

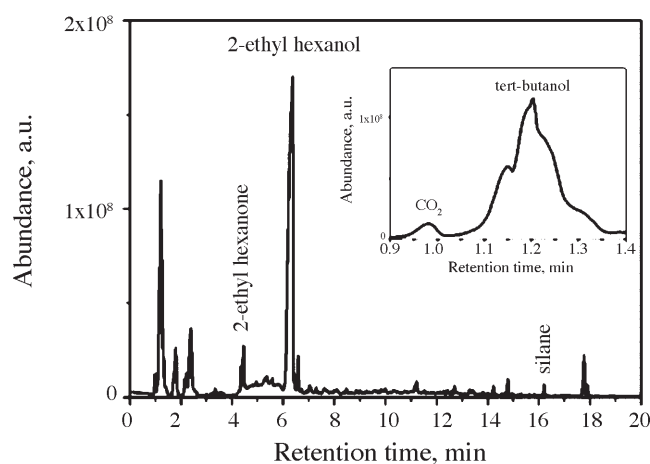
Table 1 presents a list of the main compounds identified by mass spectrometry.

The identified VOCs (**Table 1**) give a clear indication on the type of the peroxide used in this EVA formulation. Due to thermal decomposition, the peroxide undergoes homolytic bond fission, whereby the two-electron covalent bond breaks and one electron goes to each of the partner species. Tert-butanol, 2-ethyl hexanone and 2-ethyl hexanol are produced directly in the peroxide decomposition step, which also leads to the formation of two radicals as well as carbon dioxide (CO₂) as shown in **Scheme 1**. Based

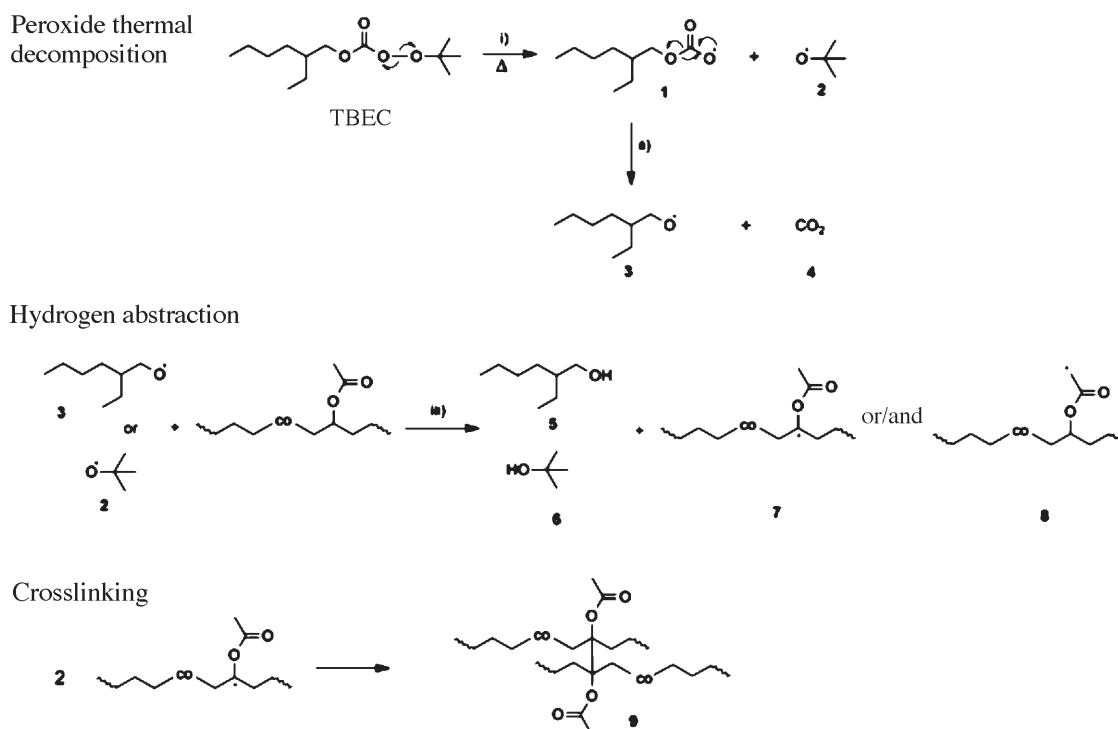
Table 1. List of the principal VOCs released from the fast-cure EVA at 160 °C

Rt [min]	Identified components
0.98	Carbon dioxide (4)
1.2	Tert-butanol (7)
1.78	Heptane
2.21	2-methyl heptane
4.34-4.43	2-ethyl hexanone
6.26-6.56	2-ethyl hexanol (5)
14.77	2-ethyl hexyl chloroformate
16.19	3-(trimethoxysilyl)propyl ester methacrylic acid (MPMA)
17.88	2,6-bis(1,1-dimethylethyl)-4-methyl-phenol (BHT)

Figure 1. GC-MS Chromatogram of VOCs collected from a fast-cure EVA at 160 °C. The insert shows the broad peak centred at about 1.2 min corresponding to tert-butanol



Scheme 1. The crosslinking process of EVA encapsulant initiated by the peroxide TBEC during the encapsulation process



on this analysis, the type of peroxide contained in this EVA formulation is determined to be *tert*-butylperoxy-2-ethylhexyl carbonate (TBEC).

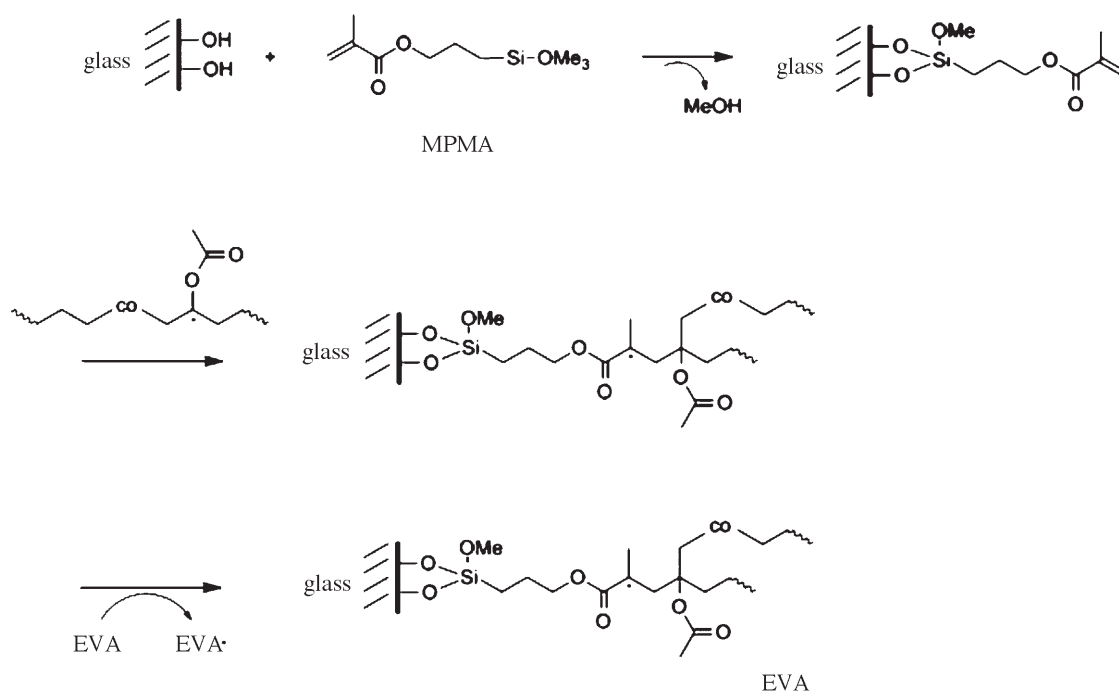
In a radical reaction, the radicals are usually generated from initiators like peroxide compounds. **Scheme 1** presents the typical scenario for the radical reaction involved in the EVA curing process. In the first step, compounds **1** as well as the radical **2** are formed *via* a homolytic scission of the peroxide O-O bond due to heat (i). Through a fast second reaction (ii) the intermediate product **1** is quickly dissociated into the peroxide **3** and carbon dioxide **4**. During the second step of hydrogen abstraction (iii), the radical **7** and/ or **8** on the EVA chain are, most likely, produced together with 2-ethyl hexanol **5** (and 2-ethyl hexanone as seen on the GC chromatogram) and *tert*-butanol **6**. The termination step leads to compound **9**, which forms the intermolecular crosslinking bonding between two EVA chains.

As shown in **Table 1**, 3-(trimethoxysilyl)propyl ester methacrylic acid (MPMA) is detected at a retention time of 16.19 mins. The MPMA is a conventional silane molecule working as the adhesion promoter in this EVA encapsulation. **Scheme 2** illustrates the principle of adhesion between EVA encapsulant and glass promoted by MPMA. The end of MPMA with 3 methanol groups is bonded to the glass surface *via* Si-O-Si chemical bonding as a result of the condensation reaction. The other end can be attacked by the radical from the peroxide dissociation and subsequently be linked to the EVA chain during the EVA curing process. The strong adhesion between EVA and glass is ensured by the fact that it is bridged with MPMA chemical bonding. However, as the Si-O-Si can experience hydrolysis under certain circumstances (e.g. moisture ingress), it is important to avoid high humidity at the interface between EVA and glass.

Besides the peroxide and the silane adhesion promoter, other compounds are also found on the GC chromatograms. Some are resulted from side reactions or degradation of the peroxide like heptanes, while others are unreacted additives formulated in EVA like phenolic derivative antioxidants (BHT) (17.88 min). A few impurities originating from the synthesis precursor of the peroxide (2-ethyl hexyl chloroformate) are also identified.

Now we will concentrate on the release of carbon dioxide as it is directly linked to the peroxide consumption, which is further related to the EVA crosslinking reaction by inferring crosslinking efficiency (namely, number of crosslinks formed per peroxide molecule decomposed). For the current analysis, CO₂ is preferred to *tert*-butanol as it is much more volatile at various collection temperatures. This ensures that all CO₂ produced during the EVA curing process will evaporate and be collected by GC-MS instead of

Scheme 2. Chemical process of the adhesion between EVA encapsulated glass with MPMA as the adhesion promote



largely dissolving into the EVA matrix. As shown in **Scheme 1**, one equivalent of peroxide gives one equivalent of CO₂. In **Figure 2** the peak area of CO₂ in the GC-MS chromatogram is plotted *versus* the different collection temperatures. The significant emission of CO₂ starts at around 100 °C. The EVA curing process is generally performed above 120 °C, when the peroxide starts to be thermally activated. The reaction rate increases rapidly at higher temperatures. A saturation plateau for CO₂ is observed around 140 °C. At this temperature we can consider that all the CO₂ has been released in the 5 mins collection time, meaning that the peroxide molecules in the EVA are wholly decomposed and the curing process has completed. In practice, the curing process of EVA encapsulants often takes place at 140 °C. This result suggests most of the EVA crosslinking bonds are created within the first 5 mins at 140 °C. Thereby, the EVA gel content develops rapidly at the beginning of the curing process and after 5 mins only slight increase in EVA gel content can be achieved by extending the EVA curing time. This conclusion coincides well with our rheological study on this EVA encapsulant and the actual encapsulation experiments performed on PV module laminators²¹. To our knowledge, it is the first time that GC-MS data has been used to follow the peroxide decomposition reaction in EVA PV encapsulants.

3.2 The Activation Energy (E_a) of the Peroxide Decomposition

The activation energy (E_a) can be obtained from the kinetic study of a chemical reaction. For determining E_a of the polymer crosslinking reaction, Differential Scanning Calorimetry (DSC) and Dynamic Mechanical Analysis (DMA) are commonly deployed²²⁻²³. In this experiment, using GC-MS techniques, it is impossible to follow the EVA crosslinking reaction kinetically as the time-evolving conversion rate is inaccessible. However, we may still

estimate the activation energy of the peroxide decomposition reaction using reasonable assumptions. The Arrhenius equation gives the dependence of the rate constant *k* of chemical reactions with the temperature *T*, as seen in Equations (1) and (2).

$$k = Ae^{\frac{E_a}{RT}} \quad (1)$$

$$\ln(k) = \ln(A) - \frac{E_a}{R} \cdot \frac{1}{T} \quad (2)$$

In which *A* is a prefactor, *E_a* is the activation energy and *R* is the gas constant.

To calculate the activation energy *E_a*, *k* has to be determined. We assume the peroxide thermal decomposition to be a first order reaction and the reaction rate to be constant throughout the whole process as shown in Equation (3):

$$\frac{d(\text{CO}_2)}{dt} = k \cdot [\text{peroxide}] \quad (3)$$

In order to calculate *k*, the concentration of peroxide and the conversion rate of CO₂ have to be determined. As aforementioned, it is reasonable to believe that all CO₂ produced in the

peroxide decomposition reaction will be evaporated, collected and trapped by the injection system of the GC-MS. As all the peroxide molecules are consumed within 5 minutes at 140 °C and 160 °C, the total amount of CO₂ can be represented by the corresponding peak area at 160 °C. Since here only the ratio between the concentration of CO₂ and the concentration of peroxide is being considered, the unit is of no importance. As the concentration of peroxide continuously decreases during the reaction, $\frac{d[\text{CO}_2]}{dt}$ is also gradually changing. To calculate *k*, the averages of $\frac{d[\text{CO}_2]}{dt}$ and of the peroxide concentration during the 5 mins collection time are used. In order to obtain the value of *E_a*, $\ln(k)$ *versus* 1/*T* is plotted in **Figure 3**. As shown in Equation (2), by taking the slope of this curve, the activation energy (E_a) of the peroxide decomposition is found to be approximately 122 kJ/mol. This is very close to the 132 kJ/mol reported in the literature²⁴. The reason why the slope of this part of the curve has been considered is as follows: the amounts of CO₂ detected at the collection temperatures below 100 °C are similar and negligible compared

Figure 2. Evolution of the abundance of carbon dioxide collected from EVA for 5 mins by GC-MS as a function of the collection temperature. Note: the plotted peak areas at all temperatures are normalized to that at 160 °C

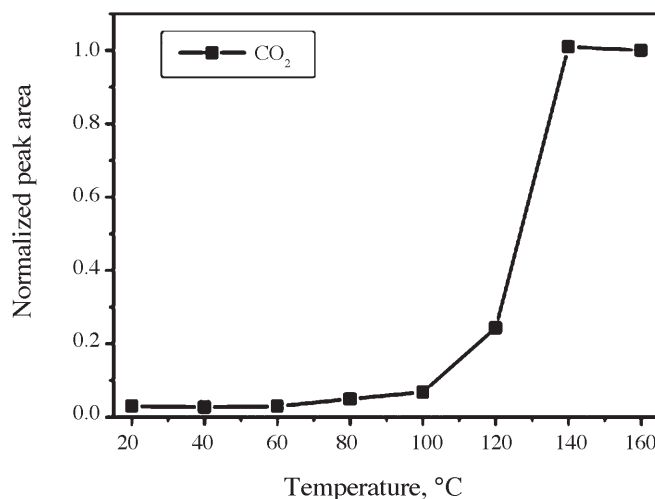


Table 2. The quantity of VOCs produced in EVA encapsulation process. The middle column shows the amount of VOCs produced by 1 g of EVA collected over 5 mins at 160 °C by GC-MS. The values in the right column are estimated for a 200MW production line, annually

Type of VOCs	Amount [mole/g]	A 200 MW line produces [kg]
CO ₂	3.8E-7	20
tert-Butanol	7.6E-6	700
Heptane,3-ethylene-	2.9E-6	400
Hexanal, 2-ethyl-	7.8E-7	120
2-ethyl hexanol	1.5E-5	2350
MPMA	1.2E-6	360
BHT	3.3E-7	80

Figure 3. Plot of $\ln(k)$ versus $1/T$. Here k is the reaction rate of the peroxide dissociation. From the slope, the activation energy (E_a) is estimated to be 122 kJ/mol

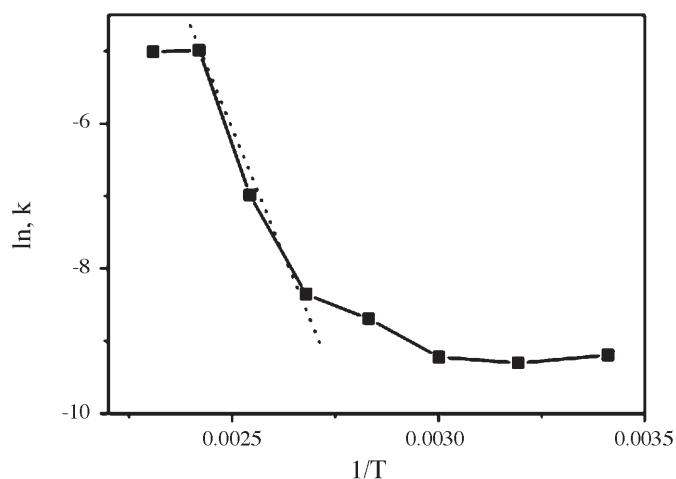
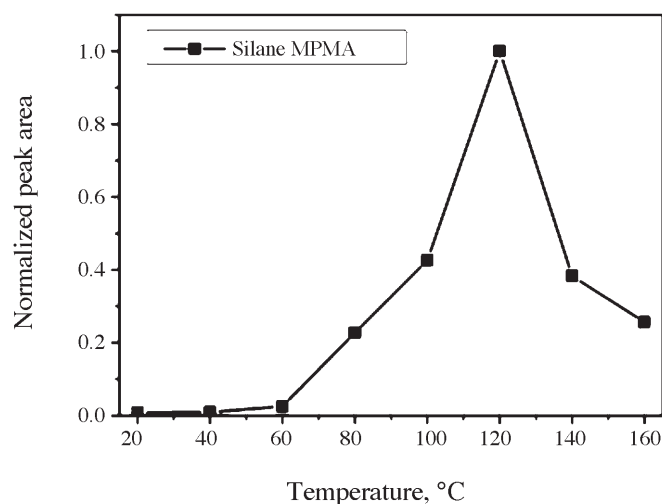


Figure 4. Evolution of the abundance of silane MPMS collected from EVA over 5 mins by GC-MS as a function of the collection temperature. Note: the plotted peak areas at all temperatures are normalized to that at 120 °C



to those collected above 100 °C. They are very likely composed of residual CO₂ in the GC column and/or the background CO₂ concentration in the GC system.

3.3 Grafting Reaction of the Silane Adhesion Promoter to the EVA Chain

As determined by GC-MS, Silane MPMA is added into this EVA formulation to promote the adhesion between EVA and glass. The amount of silane in the EVA before encapsulation will greatly influence the resulting adhesion strength, which is believed to be an important factor for judging the encapsulation quality of PV modules. In **Figure 4**, the abundance of silane MPMA, released over 5 minutes at various collection temperatures is plotted. MPMA starts to be released significantly from the EVA encapsulant at 40 to 60 °C. Practically, the glass temperature goes over 60 °C during the preheating (on pin) stage of the PV module encapsulation process. The preheating occurs in vacuum and is intended for removal of entrapped air in the EVA or in the module lay-up. That is one reason why the pressure is not applied on the module during this step. The result presented in **Figure 4** indicates that too long preheating step could cause severe loss of silane from the EVA encapsulant, which may affect the resulting adhesion strength between EVA and glass. In **Figure 4** one also notices that the released quantity of silane increases with temperature. However, this trend is reversed above 120 °C. As discussed previously, the thermal decomposition of the peroxide starts rapidly above 120 °C, and one end of the silane MPMA will be covalently bonded to the EVA chain during the crosslinking reaction. Being grafted to the EVA chain, the silane molecule will not be able to escape from the EVA matrix any more. This explains the significant drop in the detected amount of MPMA at 140 and 160 °C by GC-MS.

3.4 Environmental Impact of the EVA Encapsulation Process

The environmental impact is a very important consideration for the life cycle of products produced with polymers. It is even more important for PV modules, as PV technology is expected to be green and clean. The industry activities involving adhesives is said to play a considerable role in the emission of VOCs²⁵. As the PV module manufacturing process utilizes EVA as adhesives, the identification and estimation of the types and quantities of VOCs released from the encapsulation process are highly valuable for minimizing exposure to hazardous chemical substances.

GC-MS is a common tool for identifying the types of VOCs during the polymer processing²⁵. It could also supply quantitative information on a VOC if its response factor in the specified GC-MS setup is correctly determined by selecting a proper standard. Here, the purpose is only to roughly estimate the quantities of VOCs released from an EVA PV encapsulant during the encapsulation process, not to determine them in a strict analytical manner. Thus only one internal standard is used for the quantitative GC-MS analysis. The VOC collection is performed by heating the EVA at 160 °C for 5 mins. For simplicity, the response factor of the internal standard is used for all analyzed VOCs. The results are summarized in **Table 2**. The middle column gives the quantity of each VOC produced by 1 g of EVA during the curing process at 160 °C for 5 mins. These results allow us to estimate the overall amount of VOCs produced during PV module encapsulation processes. For a c-Si technology based PV module production line with 200 MW capacity, about 1.33 x 10⁶ m² of PV modules will be generated annually. Each module needs 2 layers of EVA with a thickness of ~0.5 mm each. That is to say, ~1330 tons of EVA will be consumed on this line in one year. Multiplying it with the

amount of VOCs per 1 g EVA (middle column) gives us the quantity of each type of VOC produced by a 200MW production line every year. The values are listed in the right column in **Table 2**. The amount of CO₂ is nearly negligible. The quantities of the other VOCs are quite considerable, like *tert*-butanol, 3-ethylene-heptane, 2-ethylhexanal, 2-ethylhexanol and MPMA. However, they fall well within the VOC emission limit for an emission source required by the Clean Air Act Amendments of 1990²⁵. BHT, with lower quantity, might cause permanent organ damage and have tumour promotion effects under long-term exposure²⁶. This result suggests that the EVA encapsulation process of PV modules is relatively clean and exhibit minor environmental impacts. But it also reinforces the necessity of having proper ventilation and exhaust treatment systems as part of the PV module production line.

4. CONCLUSIONS

The GC-MS technique is a useful tool to gain knowledge on the type and the rough amounts of VOCs produced from EVA during heating at encapsulation temperatures. This information provides unique insights into the chemistry of the EVA encapsulation process, which will be valuable for understanding and optimizing the PV module encapsulation process. Through GC-MS, the type of peroxide crosslinking initiator used in the studied EVA encapsulant is identified to be TBEC. Its decomposition kinetics is studied and the activation energy is appropriately determined to be 122kJ/mol. The temperature-dependent release of silane adhesion promoter (MPMA) is analyzed, and the result suggests a long preheating stage during EVA encapsulation may influence the adhesion between EVA and glass. This work also addresses important environmental issues. The amount of VOCs produced by a 200MW production line annually is roughly estimated using the quantitative GC-MS analysis of the EVA

encapsulant, and deemed to exhibit minor environmental impact. The evaluation of the types and quantities of these volatiles can not only help one minimize the exposure to hazardous chemical substances during PV module production, but also increase the lifetime of individual components that are part of encapsulation equipment like membranes and pumps.

ACKNOWLEDGEMENTS

The authors are grateful for continuous financial support of this project from 3S Modultec, Switzerland and the Swiss Federal Office for Energy under project 101191. The authors also thank C.F. Schlumpf for the language check.

REFERENCES

1. IMS, Quarterly PV Installation Forecasts (2011).
2. Czanderna A.W. and Pern F.J., *Sol. Ener. Mat.*, **43** (1996) 101-181.
3. Quintana M.A., King D.L., et al. *Proc. of IEEE Photovoltaic Specialists Conference*, **28** (2000) 1420-1423.
4. King D.L. and Quintana M.A., *Progress in Photovoltaics*, **8** (2000) 241-256.
5. Lewis K.J., in: C.G. Geblein, D.J. Williams, R.D. Deanin, (Eds.), *Encapsulant material requirements for photovoltaic modules in: polymers in solar energy utilization*. ACS, Washington, DC (1983): 367 - 385 (chapter 23).
6. Pern J., APP International PV reliability workshop (2008). NREL/PR-520-44666
7. Warren C., Photon International. Sept. issue (2009):292-309.
8. Pern F.J., *Angewandte Makromolekulare Chemie*, **252** (1997) 195-216.
9. El Amrani, A. Mahrane, et al. *International Journal of Photoenergy*, Vol. 2007 (2007): Article ID 27610, 5 pages. doi:10.1155/2007/27610.
10. Zahnd J. and Boos C., Machine for the production of sheet elements from composite material. WO2006128699.

11. Lange R.F.M., Luo Y., et al. *InterPV Asia*, **8** (2009) June issue.
12. Luo Y., Fidalgo I., and Lange R.F.M., *Global Solar Technology*, (2010) 14-16.
13. Lange R.F.M, Luo Y., et al. *Energetica India*, **54** (2009) July/August issue.
14. Perret-Aebi L.-E., Li H.-Y., et al. *Conference proceedings of 25th PVSEC*, Valencia (2010): 4036 - 38.
15. Wood J.R. and Bader M.G., *Compos. Manuf.*, **5** (1994) 139-47.
16. Wood J.R. and Bader M.G., *Compos. Manuf.*, **5** (1994) 149-58.
17. Costache M.C., Jiang D.D., and Wilkie C.A., *Polymer*, **46** (2005) 6947-58.
18. Mera A.E. and Snow A.W., *Journal of Applied Polymer Science*, **60** (1996) 609-16.
19. Xiang Q., Xanthos M., et al. *Polymer Degradation and Stability*, **77** (2002) 93-102.
20. Ezrin M. and Lavigne G., *Engineering Failure Analysis*, **12** (2005) 851-59.
21. Li H.-Y., Luo Y., et al. Unpublished results (2011).
22. Schubnell M., *Photovoltaics International*, (2010) 131-137.
23. Li H.-Y., Perret-Aebi L.-E. et al., *Progress in Photovoltaics*, (2011) (in press).
24. Pern F.J., *Solar Energy Materials and Solar Cells*, **41/42** (1996) 587-615.
25. Patel S.H. and Xanthos M.. *Advances in Polymer Technology*, **20** (2001) 22-41.
26. Lanigan R.S. and YamarikT.A., *Int. J. Toxicol.*, **21** (2002) 19-94.